Singlet States Open the Way to Longer Time-Scales in the Measurement of Diffusion by NMR Spectroscopy

SIMONE CAVADINI, PAUL R. VASOS

Institut des Sciences et Ingénierie Chimiques, Ecole Polytechnique Fédérale de Lausanne, EPFL, Batochime, 1015 Lausanne, Switzerland

ABSTRACT: Nuclear magnetic resonance is a powerful nonintrusive technique for measuring diffusion coefficients through the use of pulsed field gradients. The main limitation to the application range of this method is imposed by the relaxation time constants of the magnetization. The recently introduced singlet-state spectroscopy affords obtaining relaxation time constants for pairs of coupled spins which can be longer by more than an order of magnitude than the spin-lattice relaxation time constants. We review in this paper the advantages that are offered by these long relaxation time constants for diffusion measurements. Using experiments that combine singlet-state and diffusion spectroscopy, slower diffusion constants can be determined. The coupling of the two methods constitutes an alternative to the use of special probes equipped with strong gradients for the study of large molecules that diffuse slowly in solution. © 2008 Wiley Periodicals, Inc. Concepts Magn Reson Part A 32A: 68–78, 2008.

KEY WORDS: singlet-states lifetimes; slow dynamic processes; slow diffusion; nuclear magnetic resonance (NMR); large molecules

INTRODUCTION

Translational diffusion is an essential dynamic feature of molecules in liquid state and diffusion rates play a key role in chemical reactions. It is important to develop methods that provide accurate measurements of the diffusion coefficients in small sample volumes over a wide range of temperatures and molecular sizes. Nuclear magnetic resonance (NMR) spectroscopy in liquid state has the ability to probe molecular motions over a wide range of timescales (ranging from picoseconds to several seconds). These motional processes can be sampled if they affect the spin Hamiltonian: for instance, the translational motion in an inhomogeneous magnetic field changes the spin Hamiltonian as the molecules move into different regions of space.

Received 12 June 2007; revised 16 August 2007; accepted 20 August 2007

Correspondence to: Simone Cavadini; E-mail: simone.cavadini@epfl.ch

Concepts in Magnetic Resonance Part A, Vol. 32A(1) 68–78 (2008)

Published online in Wiley InterScience (www.interscience.wiley.com). DOI 10.1002/cmr.a.20100

The importance of NMR spectroscopy as a tool to study transport phenomena (diffusion, flow, convection, or electrophoretic mobility) has been increasingly recognized (*1–3*). The measurement of translational diffusion coefficients D by NMR relies on the application of gradients along one or more spatial dimensions. Investigations using pulsed field gradients (PFGs) NMR are noninvasive and can be carried out in liquid state, that is, close to physiological conditions. This makes them attractive compared to other experimental techniques used to study diffusion like ultracentrifugation, molecular sieving, neutron scattering, and quasi-elastic light scattering. An exhaustive description of the PFG-NMR technique is given in (*4*, *5*).

The relationship between diffusion coefficients D and structural properties is given by the Stokes–Einstein equation:

$$D = \frac{k_B T}{f}, \qquad [1]$$

where k_B is the Boltzmann constant, T is the temperature, and f is the friction factor. It is then possible to relate D to the Stokes radius r and the correlation time τ_c. For the simple case of a spherical particle in a medium of viscosity η:

$$f = 6\pi\eta r, \qquad [2]$$

$$\tau_c = \frac{4\pi\eta r^3}{3k_B T}. \qquad [3]$$

Since the rotational correlation time τ_c can be determined from relaxation data, this gives the possibility to obtain D from relaxation methods. Therefore, there are two distinct ways for measuring translational diffusion, the PFG-NMR experiments and the analysis of relaxation data (*4*). It is important to note that the two methods detect events occurring on two separate time scales: relaxation measurements are sensitive to motions on the picosecond or nanosecond time scale, whereas the PFG-NMR methods are sensitive to motions occurring on the time scale of milliseconds to seconds. Since deriving D from τ_c requires many assumptions regarding the relaxation mechanisms, the size and shape of the molecules, it is preferable to measure D using PFG methods. These measurements rely on observing the attenuation of a spin-echo signal caused by a combination of translational motion and known gradient pulses, which can be directly related to D. In other words, the information about the localization of molecules can be encoded and decoded by PFGs before and after a delay Δ where translational motions occur. The actual extent of this diffusion interval is limited by the time after which the spins lose phase coherence or the memory of their initial state, because of spin–spin or spin–lattice interactions. In the most elementary spin-echo experiments, the transverse relaxation time constant T_2 limits the interval where diffusion can be observed. On the other hand, if stimulated echo experiments are used, the longitudinal relaxation time constant T_1 will limit the time period during which diffusion can be allowed to take place. Since slower transport processes require longer diffusion intervals Δ, one must take into account attenuation factors that depend upon the relaxation mechanism acting during Δ. Small diffusion coefficients ($D < 10^{-10}$ m^2 s^{-1}), associated with macromolecules or supramolecular assemblies with masses larger than 50 kDa are difficult to measure with conventional methods using population or coherences subject to T_1 or T_2 relaxation processes.

As an alternative, we describe in this work a method that stores the nuclear spin order in a pair of coupled spins as a *singlet state* (*6*). This state relaxes with a time constant T_s that can be much longer than both T_1 and T_2, and which is, consequently, suitable for studying very slow transport processes. The combination of pulse sequences that excite and preserve singlet states with Diffusion-ordered spectroscopy (DOSY) leads to a new class of experiments—singlet-state diffusion spectroscopy (SS-DOSY), which are described in this article.

DOSY-TYPE EXPERIMENTS; CRITICAL PARAMETERS

DOSY experiments consist of three steps: i) coherence is excited and phase-encoded by gradients according to spatial dimensions, ii) diffusion takes place during an adjustable interval, Δ, and iii) spin order is translated into detectable coherences, phase-decoding occurring at the same time (Fig. 1). The phase-encoding is effected by PFGs and can be carried out on single-quantum coherences excited by the first 90° pulse (Fig. 1) or on higher-order coherences. A PFG can be characterized by a product:

$$\kappa = \gamma p s G_{max} \delta, \qquad [4]$$

where γ is the gyromagnetic ratio, p the coherence order, G_{max} the peak intensity of the gradient, and δ its duration. Depending on the shape of the PFG, a dimensionless shape factor $0 < s \leq 1$ can be associated to it (for instance, s is equal to 1 in case of rectangular pulses).

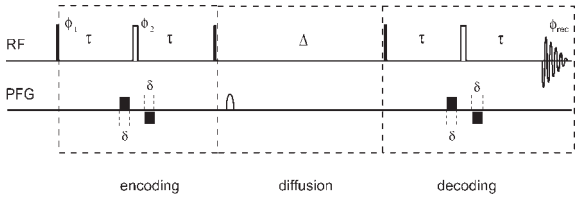

Figure 1 Pulses with flip angles of 90° and 180° are indicated by full and empty rectangles, respectively. For a system of two homonuclear J-coupled spins, one can set $\tau = 1/2J$ in order to obtain in-phase magnetisation at the end of the encoding period. The gradient durations are typically up to $\delta = 3$ ms on a normal probehead. The phase cycle is: $\phi_1 = x, -x$, $\phi_2 = 2(x), 2(-x)$, and $\phi_{rec} = x, -x$.

In Fig. 1, the decay of the observed echo signal S at the beginning of the acquisition period $\Delta + 4\tau$ is given by Eq. (1):

$$S(\kappa, \Delta) = S(0)\exp\left[-D\kappa^2(\Delta + 2\tau - 2\delta/3)\right] \times \exp(-R_2 4\tau)\exp(-R_1\Delta), \quad [5]$$

where D is the diffusion coefficient and $\Delta + 2\tau - 2\delta/3$ the effective interval between encoding and decoding by PFG, $R_{1,2} = 1/T_{1,2}$ are the longitudinal and transverse relaxation rate constants and $S(0)$ is the equilibrium magnetization. The correction factor $2\delta/3$ should be used if bipolar rectangular shape gradients are employed for the encoding and decoding steps. Other correction terms corresponding to other shapes can be found in Ref. (*7*).

With the assumption that the diffusion takes place mostly during the delay Δ (i.e., $\Delta \gg \tau, \delta$), we can describe the decay of S as:

$$S(\kappa, \Delta) = S(0)\exp\left(-D\kappa^2\Delta\right)\exp(-R\Delta), \quad [6]$$

where R is the relaxation rate constant acting during Δ.

If the signal S is observed as a function of the gradient strength and compared to a signal S_0 obtained using vanishingly small gradients, the diffusion coefficient can be fitted to the following Gaussian function given by the Stejskal–Tanner attenuation factor (*1*):

$$\frac{S}{S_0} = \exp\left(-D\kappa^2\Delta\right). \quad [7]$$

If pairs of gradients are used for the encoding and decoding steps (e.g., like in Fig. 1), a factor $2^2 = 4$ appears in Eq. [7] and the signal is attenuated in proportion to $\exp\{-D4\kappa^2\Delta\}$. The fit of the signal intensities as a function of the gradient strength using Eq. [7] provides the diffusion coefficient, D.

For slowly-diffusing molecules, it is important to increase the interval Δ in which the molecules (i.e, the spins) are allowed to diffuse to sufficiently change the spin Hamiltonian and hence make the diffusion process discernable, as can be seen from Eq. [7]. In effect, if D becomes small, one needs to increase either Δ or κ (i.e., by increasing the gradient duration or the gradient amplitude) so that the Gaussian decay may remain visible. Because of technical reasons, the gradient durations and strengths are often limited in order to avoid eddy currents or by the design of the probe. Intense PFG's can also heat the sample and damage the probe. Therefore, it is preferable to increase the diffusion delay Δ. Unfortunately, this delay is limited by the relaxation rate constant.

In Fig. 2, it is shown that longer delays Δ are needed to reveal the spatial information, as the diffusion coefficients decrease. For this purpose we define the diffusion time τ_g as the time needed by the magnetisation S defined in the Eq. [7] to decay by a factor 10 between two measuring points recorded using two gradient strengths κ_1 and κ_2, with $\kappa_1/\kappa_2 = 95/5$. From Eq. [7], it is then straightforward to get:

$$\tau_g = \frac{\ln(10)}{D(\kappa_1^2 - \kappa_2^2)}. \quad [8]$$

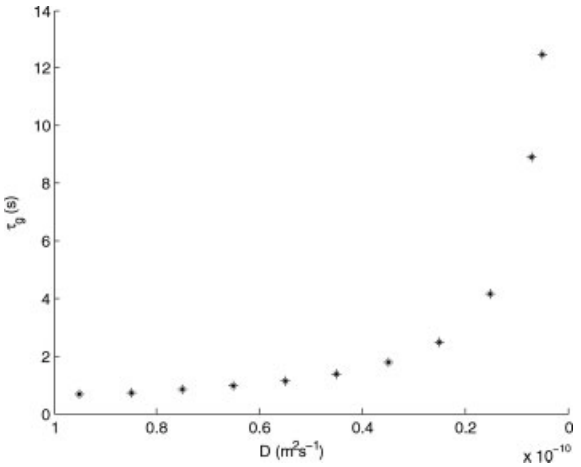

Figure 2 Appropriate delay τ_g that should be used in diffusion experiments in order to obtain a significant difference between signal intensities measured using gradient strengths κ_1 and κ_2 of 95 and 5%, as the diffusion coefficient decreases. The plot is obtained from Eq. [8]. The parameter κ is defined in Eq. [4], using: $\delta = 2$ ms, $G_{max} = 50$ G cm^{-1}, $s = 0.75$ (sine-shaped gradient pulses), $p = 1$ and $\gamma = 4258$ Hz/G for protons.

It is apparent from Fig. 2 that the smaller the diffusion coefficient D, the longer the delay τ_g that is needed to perform a reliable fit using Eq. [7]. Therefore, the relaxation rate constant of the system has to allow for the use of such long delays, i.e., it has to be as small as possible. The use of singlet states achieves this requirement by quenching one of the main mechanisms that lead to relaxation in a pair of coupled spins, the dipolar interaction. In other words, a necessary condition to obtain reliable fits is that the relaxation rate constant R of the magnetization in Eq. [6] be smaller or comparable to the product of the diffusion coefficient, D, and κ^2. Figure 3 illustrates the decay of the intensity as a function of the diffusion interval Δ for two cases, one when R is comparable to $\kappa^2 D$ and one when R is an order of magnitude larger. It can be seen clearly that in the first case it is straightforward to choose a delay Δ for which the difference between the signals recorded using 5 and 95% of the gradient strength is significant. In the second case, the difference between the signals recorded with the two gradient strengths is smaller, and therefore it will be more difficult to determine the diffusion coefficient from a fit of the signal intensity as a function of the gradient strength using Eq. [7].

Moreover, using coherences that have low relaxation rate constants R, such as the singlet state, one is also able to better discriminate between different molecular masses M. The difference between the signal intensities in experiments recorded using 5 and 95% of G_{max} for two different diffusion coefficients is larger for longer delays, provided that the signals are not affected by relaxation. The two diffusion coefficients D_1 and D_2 for which the decays were plotted in Fig. 3 correspond to molecular masses in a ratio $M_2/M_1 = ½$, with $M_1 \sim 50$ kDa [using Eqs. [1]–[3] and with the assumption that τ_c (ps) $\approx M$ (Da) (*8*)]. It can be seen that, the lower the relaxation rate constants the longer the delays Δ for which relaxation phenomena induce significant losses, independently of the diffusion coefficients. The optimum values Δ^{opt} for the delays Δ, i.e., long enough for diffusion to become manifest, but short enough so the relaxation does not spoil the signal, are indicated by arrows in Fig. 3. Experimental techniques giving lower relaxation rate constants, such as singlet-state spectroscopy, are needed in order to use longer delays Δ, and, consequently, to obtain a contrast between different diffusion coefficients.

Singlet State Theory

In the previous section we showed that smaller relaxation rate constants are beneficial for the study of diffusion. In NMR, the relaxation rate constants R_1, which describe the return to equilibrium of longitudinal magnetization, are smaller than the relaxation rate constants R_2, which describe the decay of transverse magnetization. Therefore, the first approach to take in order to ensure that the excited magnetization decays slowly is to use longitudinal magnetization during the diffusion interval (as $R_1 < R_2$). Another approach that reduces the relaxation rate constants of the diffusing species is the transfer of magnetization to hetero-

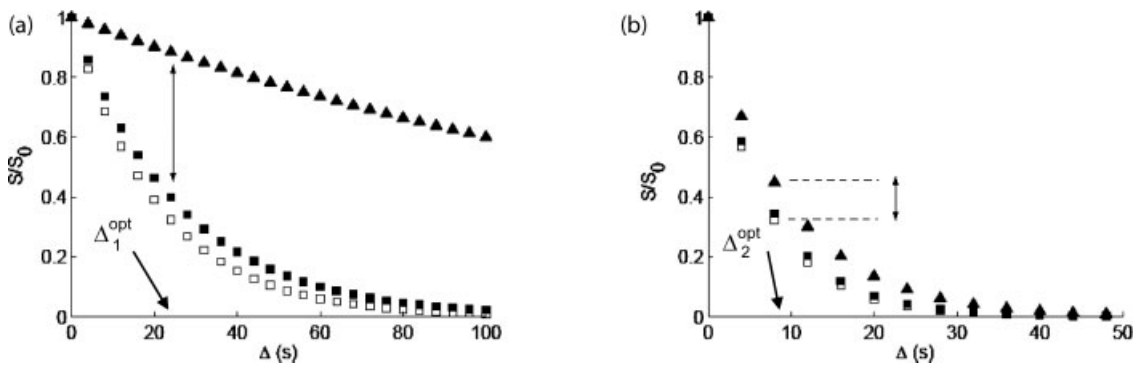

Figure 3 Decay of signal intensities simulated with Eq. [6] as a function of the diffusion interval, Δ, for two different gradients with strengths of 5% (triangles) and 95% (squares) of G_{max}, respectively. The parameters were $\delta = 0.6$ ms, $G_{max} = 50$ G cm^{-1}, $s = 0.75$, $p = 1$, and $\gamma = 4258$ Hz/G. The diffusion coefficients are chosen as $D_1 = 10^{-11}$ m^2 s^{-1} (filled symbols) and $D_2 = 1.3 \times 10^{-11}$ m^2 s^{-1} (open symbols), with $\kappa^2 D_1 = 0.03$ s^{-1} and $\kappa^2 D_2 = 0.04$ s^{-1}, for the gradients at 95% of G_{max}. In (a) the relaxation rate constant is $R = 0.01$ s^{-1}, while in (b) we show the decays for $R = 0.1$ s^{-1}. The arrows indicate the optimum delays, $\Delta_1^{opt} = 24$ s and $\Delta_2^{opt} = 8$ s, that should be used for distinguishing between the two diffusion coefficients, D_1 and D_2, in a PFG experiment.

nuclei that have smaller relaxation rate constants because of their reduced gyromagnetic ratio (*9–12*). This approach is particularly effective, as the low gyromagnetic ratios of heteronuclei scale down all dipolar interactions, including those with electronic spins. The use of low-gamma nuclei to increase the lifetimes of spin-order has been predicted to be effective in both paramagnetic and large molecules, and can be introduced in experiments with direct excitation and detection of heteronuclei (*13*, *14*).

The mechanisms that lead to relaxation are the dipolar interaction of the concerned spins with other nuclear or electronic spins and fluctuations of the chemical shift anisotropy because of molecular motion. For protons, the dipolar interaction represents the main contribution to both transverse and longitudinal relaxation rate constants, as the chemical shift anisotropies are negligible.

The dipolar contributions to relaxation are inversely proportional to the sixth power of the distance between the involved spins, so the most important ones arise from pairs of spins which are closest in space; some of the pairs of spins in this situation are also *J*-coupled. If a molecule contains two magnetic nuclei I and S with a nonvanishing coupling J_{IS}, it has been shown (*6*) that the relaxation contribution to the dipolar interaction between spins I and S is innocuous to the so-called singlet states (SS), i.e., linear combinations of product states that are antisymmetric with respect to the permutation of the two spins ($|S_0\rangle = N\{|\alpha\beta\rangle - |\beta\alpha\rangle\}$, with $N = 2^{-1/2}$). In this case, we may speak of a singlet-state relaxation rate constant R_s or, alternatively, of a singlet-state relaxation time constant $T_s = 1/R_s$.

The more isolated the pair of coupled spins is from other (external) spins, the longer its lifetime T_s. This is due to the fact that the singlet configuration cancels the effects of the dipolar interaction between the two spins, while dipolar interactions with external spins scale down the T_s lifetime. Therefore, there exists an a priori limiting requirement that the spins on which singlet states are created be isolated from interactions with external spins (e.g., by creating singlet states on protons and deuterating the close neighbors). This requirement might not be as strict as originally believed, as recent research has shown that long-lived spin states can be sustained in spin systems with more than two spins (*15*, *16*) and that the presence of J-couplings with external spins does not diminish the lifetime of the singlet state created on two spins that have a sufficiently strong intra-pair J-coupling (*17*).

In order for singlet states to become eigenstates of the system (i.e., in order to prevent them from mixing with other faster-relaxing states during coherent evolution) a strong radio-frequency field must be applied. For CW irradiation, the main condition is that the decoupling amplitude ν_1 should be considerably larger than the chemical shift difference between the two spins $\Delta\nu_{IS} = \nu_I - \nu_S$ (*18*, *19*). The efficiency of the decoupling can be increased through the use of composite pulses (*20*) or of shaped pulses (*21*). Under strong decoupling, a two-spin system has four eigenstates (*20*, *22*):

$$|S_0\rangle = N\{|\alpha_I\beta_S\rangle - |\beta_I\alpha_S\rangle\} \quad [9]$$

$$|T_{+1}\rangle = |\alpha_I\alpha_S\rangle,$$

$$|T_0\rangle = N\{|\alpha_I\beta_S\rangle + |\beta_I\alpha_S\rangle\},$$

$$|T_{-1}\rangle = |\beta_I\beta_S\rangle.$$

Consider the matrix V that converts the product base:

$$\Phi_{PB} = \{|\alpha\alpha\rangle, |\alpha\beta\rangle, |\beta\alpha\rangle, |\beta\beta\rangle\}, \quad [10]$$

into the singlet-triplet space base:

$$\Phi_{STB} = \{|T_{+1}\rangle, |T_0\rangle, |S_0\rangle, |T_{-1}\rangle\}, \quad [11]$$

so that:

$$\Phi_{PB} = V \cdot \Phi_{STB}. \quad [12]$$

The Cartesian operator products frequently used for calculating coherence transfer processes in the Φ_{PB}-related Liouville space (*23*) can be transformed into the symmetry-related STB space:

$$B_{STB} = VB_{PB}V^{-1} \quad [13]$$

The conversion table (Table 1) contains, in the second column, the operators of the Φ_{STB}-related Liouville space that give a measure of the expectation values of the populations of the singlet state ($p(S_0) = |S_0\rangle\langle S_0|$) and of the three triplet states ($p(T_{+1}) = |T_{+1}\rangle\langle T_{+1}|$, etc.), as well as coherences between these states that are produced by switching the irradiating field on at the moment when the coherences in the Φ_{PB}-related Liouville space are described by operators in the first column. In Fig. 4 it is exemplified how this conversion takes place. It can be seen that only certain product operators in the Liouville space associated with Φ_{PB} lead to nonzero differences of populations between the singlet-state S_0 and the three triplet states in Φ_{STB}.

Table 1 Conversion of Operators Between the Liouville Spaces Associated to the Product Base Φ_{PB} and the Singlet-triplet Base Φ_{STB}

Operator in the Liouville space associated to Φ_{PB}	Operator in the Liouville space associated to Φ_{STB}
$\frac{E}{2}$	$\frac{1}{2}(\|T_{+1}\rangle\langle T_{+1}\| + \|T_0\rangle\langle T_0\| + \|S_0\rangle\langle S_0\| + \|T_{-1}\rangle\langle T_{-1}\|)$
I_x	$\frac{1}{2\sqrt{2}}(\|T_{+1}\rangle\langle T_0\| - \|T_{+1}\rangle\langle S_0\| + \|T_0\rangle\langle T_{+1}\| + \|T_0\rangle\langle T_{-1}\| - \|S_0\rangle\langle T_{+1}\| + \|S_0\rangle\langle T_{-1}\| + \|T_{-1}\rangle\langle T_0\| + \|T_{-1}\rangle\langle S_0\|)$
I_y	$\frac{i}{2\sqrt{2}}(\|T_{+1}\rangle\langle T_0\| - \|T_{+1}\rangle\langle S_0\| - \|T_0\rangle\langle T_{+1}\| + \|T_0\rangle\langle T_{-1}\| + \|S_0\rangle\langle T_{+1}\| - \|S_0\rangle\langle T_{-1}\| - \|T_{-1}\rangle\langle T_0\| - \|T_{-1}\rangle\langle S_0\|)$
I_z	$\frac{1}{2}(\|T_{+1}\rangle\langle T_{+1}\| + \|T_0\rangle\langle S_0\| + \|S_0\rangle\langle T_0\| - \|T_{-1}\rangle\langle T_{-1}\|)$
S_x	$\frac{1}{2\sqrt{2}}(\|T_{+1}\rangle\langle T_0\| + \|T_{+1}\rangle\langle S_0\| + \|T_0\rangle\langle T_{+1}\| + \|T_0\rangle\langle T_{-1}\| + \|S_0\rangle\langle T_{+1}\| - \|S_0\rangle\langle T_{-1}\| + \|T_{-1}\rangle\langle T_0\| - \|T_{-1}\rangle\langle S_0\|)$
S_y	$\frac{i}{2\sqrt{2}}(\|T_{+1}\rangle\langle T_0\| + \|T_{+1}\rangle\langle S_0\| - \|T_0\rangle\langle T_{+1}\| + \|T_0\rangle\langle T_{-1}\| - \|S_0\rangle\langle T_{+1}\| - \|S_0\rangle\langle T_{-1}\| - \|T_{-1}\rangle\langle T_0\| + \|T_{-1}\rangle\langle S_0\|)$
S_z	$\frac{1}{2}(\|T_{+1}\rangle\langle T_{+1}\| - \|T_0\rangle\langle S_0\| - \|S_0\rangle\langle T_0\| - \|T_{-1}\rangle\langle T_{-1}\|)$
$2I_xS_z$	$\frac{1}{2\sqrt{2}}(\|T_{+1}\rangle\langle T_0\| - \|T_{+1}\rangle\langle S_0\| + \|T_0\rangle\langle T_{+1}\| - \|T_0\rangle\langle T_{-1}\| - \|S_0\rangle\langle T_{+1}\| - \|S_0\rangle\langle T_{-1}\| - \|T_{-1}\rangle\langle T_0\| - \|T_{-1}\rangle\langle S_0\|)$
$2I_yS_z$	$\frac{i}{2\sqrt{2}}(\|T_{+1}\rangle\langle T_0\| - \|T_{+1}\rangle\langle S_0\| - \|T_0\rangle\langle T_{+1}\| - \|T_0\rangle\langle T_{-1}\| + \|S_0\rangle\langle T_{+1}\| - \|S_0\rangle\langle T_{-1}\| + \|T_{-1}\rangle\langle T_0\| + \|T_{-1}\rangle\langle S_0\|)$
$2I_zS_x$	$\frac{1}{2\sqrt{2}}(\|T_{+1}\rangle\langle T_0\| + \|T_{+1}\rangle\langle S_0\| + \|T_0\rangle\langle T_{+1}\| - \|T_0\rangle\langle T_{-1}\| + \|S_0\rangle\langle T_{+1}\| + \|S_0\rangle\langle T_{-1}\| - \|T_{-1}\rangle\langle T_0\| + \|T_{-1}\rangle\langle S_0\|)$
$2I_zS_y$	$\frac{i}{2\sqrt{2}}(\|T_{+1}\rangle\langle T_0\| + \|T_{+1}\rangle\langle S_0\| - \|T_0\rangle\langle T_{+1}\| - \|T_0\rangle\langle T_{-1}\| - \|S_0\rangle\langle T_{+1}\| + \|S_0\rangle\langle T_{-1}\| + \|T_{-1}\rangle\langle T_0\| - \|T_{-1}\rangle\langle S_0\|)$
$2I_zS_z$	$\frac{1}{2}(\|T_{+1}\rangle\langle T_{+1}\| - \|T_0\rangle\langle T_0\| - \|S_0\rangle\langle S_0\| + \|T_{-1}\rangle\langle T_{-1}\|)$
ZQ_x	$\frac{1}{2}(\|T_0\rangle\langle T_0\| - \|S_0\rangle\langle S_0\|)$
ZQ_y	$\frac{i}{2}(-\|T_0\rangle\langle S_0\| + \|S_0\rangle\langle T_0\|)$
DQ_x	$\frac{1}{2}(\|T_{+1}\rangle\langle T_{-1}\| + \|T_{-1}\rangle\langle T_{+1}\|)$
DQ_y	$\frac{i}{2}(-\|T_{+1}\rangle\langle T_{-1}\| + \|T_{-1}\rangle\langle T_{+1}\|)$

To obtain a coherence with a minimal relaxation rate constant during the diffusion interval, the spin system must be prepared in a state that maximizes the difference between the population of the singlet state and the mean population of the triplet states (*17*). This preparation, as well as the spatial phase-encoding of the magnetization is performed prior to the diffusion period Δ (Fig. 5).

The normalized operator that corresponds to a maximum difference between the populations of $|S_0\rangle$ and the mean population of the other three states of Φ_{STB} is (*17*):

$$Q_{LLS} = \frac{\sqrt{3}}{2}\left[|S_0\rangle\langle S_0| - \frac{1}{3}(|T_{+1}\rangle\langle T_{+1}| + |T_0\rangle\langle T_0| + |T_{-1}\rangle\langle T_{-1}|)\right]. \quad [14]$$

When the Liouvillian that describes the evolution of the two coupled spins under irradiation is diagonalized, the operator Q_{LLS} is one of the eigenvectors, and its eigenvalue, λ_{LLS}, describes the decay rate constant of the difference in populations between singlet and triplet states (*17*). The characteristic time constant of the decay of the singlet-state population to equilibrium, T_s, is the inverse of this eigenvalue, $T_s = 1/\lambda_{LLS}$.

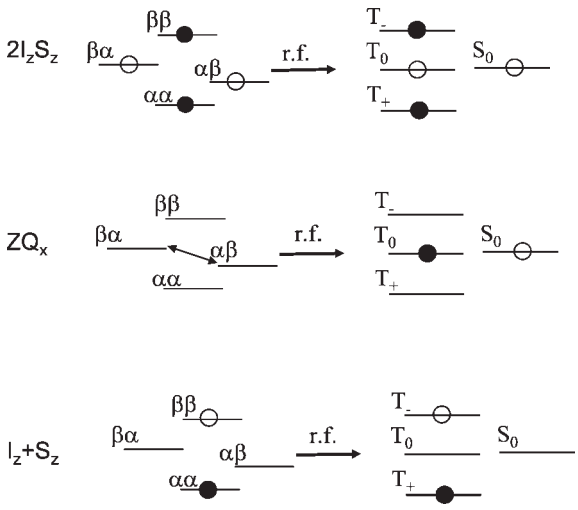

Figure 4 Example of inter-conversions of populations and coherences between the Liouville spaces corresponding to Φ_{PB} and Φ_{STB}. Filled circles indicate populations in excess with respect to the demagnetised state, arrows indicate coherences.

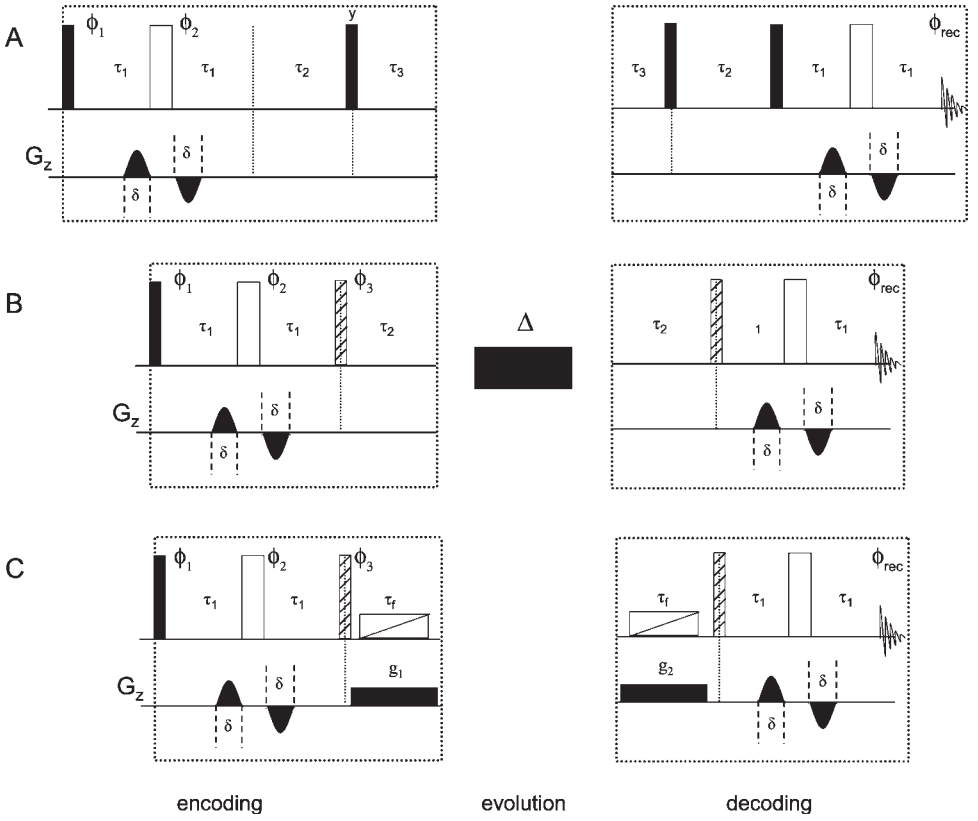

Figure 5 Pulse sequences for singlet-state diffusion spectroscopy (SS-DOSY). Open, filled, and hatched rectangles represent 180°, 90°, and 45° pulses, respectively. The rectangles with diagonal bars during the delays τ_f represent adiabatic frequency-swept pulses applied in conjunction with PFGs g_1 and g_2 (black rectangles) in order to suppress zero-quantum coherences (*24*). The delays must be adjusted to the offsets ν_I and ν_S of spins I and S and to the coupling constant J_{IS}: $\tau_1 = 1/(4J_{IS})$, $\tau_2 = 1/[2(\nu_I - \nu_S)]$, and $\tau_3 = \tau_2/2$. Sequence A also requires that the carrier frequency, ν_{RF}, be set half-way between the two chemical shifts, $\nu_{RF} = (\nu_I + \nu_S)/2$. The phase cycle for A is: $\phi_1 = x,-x$, $\phi_2 = 2(x)$, $2(-x)$, and $\phi_{rec} = (x,-x)$. The phase cycle for B and C is: $\phi_1 = x,-x$, $\phi_2 = 2(x)$, $2(-x)$, $\phi_3 = 4(y)$, $4(-y)$, and $\phi_{rec} = 2(x, -x)$, $2(-x,x)$.

Using the conversion formulae in Table 1, one obtains for the normalized operator Q_{LLS} (*25*):

$$Q_{\mathrm{LLS}} = -\frac{2}{\sqrt{3}}\left(I_xS_x + I_yS_y + I_zS_z\right) = -\frac{2}{\sqrt{3}}\vec{I}\cdot\vec{S}. \quad [15]$$

The encoding sequence is constructed in a manner that maximizes the projection of the operator present at the end of this period on Q_{LLS} (Fig. 5). From Table 1 and Eq. [15] it can be seen that there are three ways of achieving that, i.e., exciting zero-quantum coherence $ZQ_x = I_xS_x + I_yS_y$, longitudinal two-spin order I_zS_z, or both. Methods to achieve these three possibilities are presented in Fig. 5. Usually, the decoding sequence can be constructed from the mirror image of the encoding step.

Sequence A in Fig. 5 corresponds to the method developed by Carravetta and Levitt to excite singlet states (*18*). The operator that is excited (and phase-encoded) at the beginning of the diffusion period Δ is, with this method:

$$Q_{\mathrm{A}} = -2\mathrm{ZQ}_x = |S_0\rangle\langle S_0| - |T_0\rangle\langle T_0|. \quad [16]$$

Using sequence B in Fig. 5, transverse single-quantum coherence is excited and phase encoded, to be transformed, at the beginning of the diffusion period (*20*), into:

$$\begin{aligned} Q_{\mathrm{B}} &= -\mathrm{ZQ}_x - 2I_zS_z \\ &= |S_0\rangle\langle S_0| - \frac{1}{2}(|T_{+1}\rangle\langle T_{+1}| + |T_{-1}\rangle\langle T_{-1}|). \end{aligned} \quad [17]$$

It can be seen that both operators Q_A and Q_B have the same projection on Q_{LLS}:

$$P_A = \mathrm{Tr}\left(Q'_A \cdot Q_{LLS}\right) = P_B = \mathrm{Tr}\left(Q'_B \cdot Q_{LLS}\right) = \frac{2}{\sqrt{3}}. \quad [18]$$

Therefore, the same amount of long-lived order is produced at the beginning of the evolution period Δ by sequences A and B. The only difference between the two sequences is that, with sequence B, the position of the carrier, ν_{RF}, does not need to be adapted to the Larmor frequencies of the two spins, ν_I and ν_S (see Fig. 5). In this way, the range of chemical shifts (and therefore the range of molecules) amenable to diffusion studies is broader.

Making use of sequence C in Fig. 5, one obtains at the beginning of the evolution period (*20*):

$$Q_C = -2I_zS_z = \frac{1}{2}(|S_0\rangle\langle S_0| + |T_0\rangle\langle T_0| - |T_{+1}\rangle\langle T_{+1}| - |T_{-1}\rangle\langle T_{-1}|). \quad [19]$$

The projection of operator Q_C on Q_{LLS} is:

$$P_C = Tr\left(Q'_C \cdot Q_{LLS}\right) = \frac{1}{\sqrt{3}} = \frac{P_A}{2} = \frac{P_B}{2}. \quad [20]$$

The method using pulse sequence C in Fig. 5 is therefore less sensitive than those using sequences A and B, but its advantage, due to the suppression of ZQ_x coherence by the method of Thrippleton and Keeler (*24*), is that it does not depend on the relative positions of the resonances of spins *I* and *S* (since it does not contain any delay $\tau_2 = 1/[2(\nu_I - \nu_S)]$), and therefore it can be applied to pairs of spins irrespective of their resonance positions, as long as effective irradiation during the delay Δ can be achieved (*21*).

After the evolution period, the Q_{LLS} operator is converted back into single-quantum coherences and phase-decoding is performed using the last two PFGs (Fig. 5). It should be noted that another factor two in sensitivity is lost in sequence C with respect to sequences A and B during this third step, as the ZQ_x coherence is again suppressed after the diffusion period, thus making pulse sequence C four times less sensitive than the other two.

Studies of Diffusion via Singlet States

It has been shown that a singlet state can be generated for a pair of homonuclear coupled spins in many different molecular systems (*18*, *20*). We are going to exemplify the use of the combined singlet-state and diffusion spectroscopy methods showing results obtained on 2-chloroacrylonitrile ($H_IH_SC{=}CRR'$ with R = Cl and R′ = CN). The two spins I and S for which the singlet state is created are the two protons dubbed H_I and H_S. This molecule has been already used by us for diffusion measurements using singlet states and the spin-lattice relaxation time constants T_1, as well as the singlet-state lifetimes T_s, are known for this compound over a wide range of temperatures (*26*).

As it has been shown in the preceding chapters, if the diffusion coefficients become smaller, longer diffusion times Δ or stronger gradients (larger κ-values) are needed for accurate fitting of the diffusion constants. Using singlet state diffusion spectroscopy sequences (Fig. 5), the delays Δ can be extended at least up to the lifetime of the singlet state ($\Delta < T_s$). Figure 6 shows a comparison between the Gaussian decay of the proton signal intensity obtained using a standard stimulated echo sequence (Fig. 1), and the decay obtained with the singlet state sequence (SS-SQ-DOSY, Fig. 5a) at two different temperatures, 254 and 245 K, respectively. The signals are attenuated in proportion to $\exp\{-D4\kappa^2\Delta\}$, as expressed in Eq. [7] (the factor $2^2 = 4$ is a consequence of the bipolar pulse pairs, i.e., of the fact that pairs of PFGs are used, rather than single gradients). At 254 K, $T_s \approx 20$ s and $T_1 \approx 2$ s, whereas at 245 K, $T_s \approx 13$ s and $T_1 \approx 1.2$ s. In Figs. 6(b, d) it is shown that it was possible to set Δ as long as the lifetime of the singlet state, T_s, at both temperatures, and hence to considerably reduce the factors κ (on the abscisae) compared to an experiment run at the same temperature with the conventional stimulated echo sequence [Figs. 6(a, c)].

The delays Δ that could be chosen in the two examples shown in Figs. 6(b, d), using singlet-state coherences, are an order of magnitude larger than the delays that were used for longitudinal magnetisation [Figs. 6(a, c)]. Therefore, the gradient lengths, δ, used in the singlet-state diffusion sequence (Fig. 5a) were significantly smaller than those needed for the determination of the same diffusion coefficients via the classical DOSY experiment using stimulated echoes (Fig. 1).

The reduction of the necessary gradient durations, δ, and their peak intensities, G_{max}, is of critical importance in view of applications for the measurement of slow diffusion coefficients. Indeed, the inherent technical limitations on these parameters make the applications of DOSY experiments to slowly diffusing systems difficult. The product $b = \kappa^2 \cdot \Delta$ is the critical factor that determines the minimum diffusion coefficient *D* that can be fitted from data obtained from a PFG-NMR experiment, i.e., the lower *D* the higher the required values for *b*. The development of SS-DOSY makes it possible to use the available gradient durations and strengths for the study of slowly

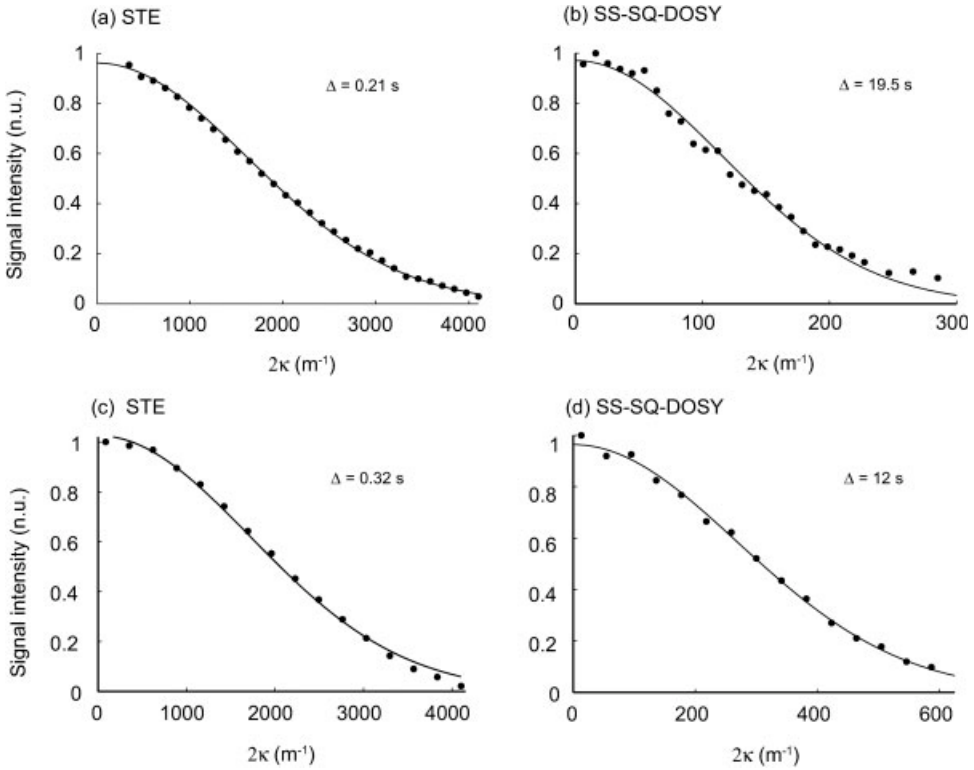

Figure 6 Experimental decays of the proton signal intensities in a 10 mM sample of 2-chloroacrylonitrile in DMSO[D_6]/D_2O (molar ratio 1:3), measured at 300 MHz and obtained with (a) the conventional STE sequence at 254 K, (b) the SS-SQ-DOSY sequence (Fig. 5a) at 254 K, (c) the STE sequence at 245 K and (d) the SS-SQ-DOSY sequence at 245 K. The parameter κ is defined in Eq. [4]. It was possible to measure the diffusion coefficient D using $\delta = 2$ ms in (a), $\delta = 155$ μs in (b), $\delta = 2$ ms in (c), and $\delta = 310$ μs in (d). The fitted diffusion coefficients at the two temperatures were (a) $D = (1.1 \pm 0.3) \times 10^{-10}$ m^2 s^{-1}, (b) $D = (1.9 \pm 0.6) \times 10^{-10}$ m^2 s^{-1}, (c) $D = (6 \pm 0.2) \times 10^{-11}$ m^2 s^{-1}, and (d) $D = (5.7 \pm 0.2) \times 10^{-11}$ m^2 s^{-1}. The diffusion intervals Δ that were used are shown in each of the plots (a)–(d).

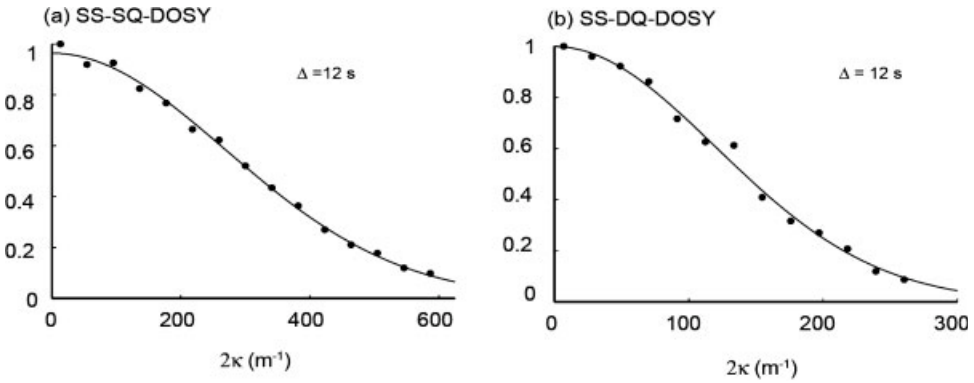

Figure 7 Experimental decays of the proton signal intensities in a 10 mM sample of 2-chloroacrylonitrile in DMSO[D_6]/D_2O (molar ratio 1:3) measured at 300 MHz and 245 K and obtained with (a) the SS-SQ-DOSY sequence and (b) with the SS-DQ-DOSY sequence. Note the scales of the abscissae, showing the parameter κ (the factor 2 describes the bipolar gradients in the encoding and decoding steps).

diffusing species, such as large molecules, molecules of nonspherical shape with large radii of gyration [such as unfolded molecules and molten globules (*27*)] or tumbling in highly viscous media, resembling the interior of the cells (*28*); it is also often the case of supramolecular assemblies (*29*).

A further reduction in the required gradient duration (or strength) can be obtained by phase-encoding a spin coherence of a higher order in the first step of a diffusion experiment (Fig. 1). This also applies to singlet-state diffusion experiments. Indeed, it has been shown by Cavadini et al. (*26*) that it is possible to excite the singlet state with a sequence called *singlet-state double-quantum DOSY* (SS-DQ-DOSY), where the encoding and the decoding steps are applied to double-quantum coherences. Figure 7 shows the advantage of the SS-DQ-DOSY method. Since the parameter κ is directly proportional to the coherence order p and the gradient length δ (Eq. [4]), using the SS-DQ-DOSY sequence it has been possible to run the same diffusion measurement with a gradient length δ that is half as long compared to the length δ used for with the SS-SQ-DOSY sequence.

CONCLUSIONS

This work describes the advantages that can be obtained by combining singlet-state spectroscopy with DOSY techniques for the study of diffusion coefficients. The scope of DOSY can be significantly extended by the use of diffusion intervals going up to the limit afforded by the long relaxation time constants, T_s, of singlet states. A theoretical description of adequate methods for obtaining singlet states for pairs of coupled spins during the diffusion interval is provided.

Diffusion coefficients of slowly-diffusing molecules in solution can be measured accurately using singlet-state spectroscopy, thus reducing the required gradient durations and amplitudes and circumventing the need to use special probeheads with high gradient strengths. SS-DOSY sequences should be used in cases when the longitudinal relaxation time constant T_1 becomes too short and limits the applicability of conventional stimulated-echo sequences. Either single- or double-quantum encoding can be implemented in SS-DOSY, the second option allowing for a further reduction of the required gradient durations or strengths by a factor of two.

The possible applications of SS-DOSY extend to all systems having low diffusion coefficients, such as large molecules, species in highly viscous media, unfolded proteins, and nucleic acids of irregular shape and with large radii of gyration.

ACKNOWLEDGMENTS

The authors thank Geoffrey Bodenhausen for his support and for many useful suggestions. We also wish to thank Riddhiman Sarkar for stimulating discussions and Martial Rey for technical assistance. This work was funded by the Swiss National Science Foundation (FNRS), the Ecole Polytechnique Fédérale de Lausanne (EPFL), and the Swiss Commission for Technology and Innovation (CTI). We are indebted to Malcolm Levitt for providing us with the manuscript of Ref. *17* prior to publication.

REFERENCES

1. Stejskal EO, Tanner JE. 1965. Spin diffusion measurements—spin echoes in presence of a time-dependent field gradient. J Chem Phys 42:288–292.
2. Kivelson D. 1977. Molecular motions in liquids introductory review and analysis: a hydrodynamic slant. Faraday Symp Chem Soc 11:7–25.
3. Johnson C. 1998. Diffusion ordered nuclear magnetic resonance spectroscopy: principles and applications. Progr Nucl Magn Reson Spectros 34:203–256.
4. Price WS. 1997. Pulsed-field gradient nuclear magnetic resonance as a tool for studying translational diffusion. I. Basic theory. Concepts Magn Reson 9: 299–336.
5. Price WS. 1998. Pulsed-field gradient nuclear magnetic resonance as a tool for studying translational diffusion. II. Experimental aspects. Concepts Magn Reson 10:197–237.
6. Carravetta M, Johannessen OG, Levitt MH. 2004. Beyond the T_1 limit: singlet nuclear spin states in low magnetic fields. Phys Rev Lett 92:153003–153004.
7. Price WS, Kuchel PW. 1991. Effect of nonrectangular field gradient pulses in the stejskal and tanner (diffusion) pulse sequence. J Magn Reson 94:133–139.
8. Hore P. 1995. Nuclear Magnetic Resonance. Oxford: Oxford University Press.
9. Orekhov VY, Korzhnev DM, Pervushin KV, Hoffmann E, Arseniev AS. 1999. Sampling of protein dynamics in nanosecond time scale by N-15 NMR relaxation and self-diffusion measurements. J Biomol Struct Dynam 17:157–174.
10. Choy WY, Mulder FAA, Crowhurst KA, Muhandiram DR, Millett IS, Doniach S, Forman-Kay JD, Kay LE. 2002. Distribution of molecular size within an unfolded state ensemble using small-angle X-ray scattering and pulse field gradient NMR techniques. J Mol Biol 316:101–112.

11. Ferrage F, Zoonens M, Warschawski DE, Popot JL, Bodenhausen G. 2003. Slow diffusion of macromolecular assemblies by a new pulsed field gradient NMR method. J Am Chem Soc 125:2541–2545.
12. Wenter P, Bodenhausen G, Dittmer J, Pitsch S. 2006. Kinetics of RNA refolding in dynamic equilibrium by ^{1}H-Detected ^{15}N exchange NMR spectroscopy. J Am Chem Soc 128:7579–7587.
13. Bertini I, Duma L, Felli IC, Fey M, Luchinat C, Pierattelli R, et al. 2004. A heteronuclear direct-detection NMR spectroscopy experiment for protein-backbone assignment. Angew Chem Int Ed 43:2257–2259.
14. Bermel W, Bertini I, Duma L, Felli IC, Emsley L, Pierattelli R, Vasos PR. 2005. Complete assignment of heteronuclear protein resonances by protonless NMR spectroscopy. Angew Chem Int Ed 44:3089–3092.
15. Pileio G, Concistrè M, Carravetta M, Levitt MH. 2006. Long-lived nuclear spin states in the solution NMR of four-spin systems. J Magn Reson 182:353–357.
16. Vinogradov E, Grant AK. 2007. Long-lived states in solution NMR: selection rules for intramolecular dipolar relaxation in low magnetic fields. J Magn Reson 2007; 188:176–182. doi:10.1016/j.jmr.2007.05. 015.
17. Pileio G, Levitt MH. 2007. J-Stabilization of singlet states in the solution NMR of multiple-spin systems. J Magn Reson 187:141–147.
18. Carravetta M, Levitt MH. 2004. Long-lived nuclear spin states in high-field solution NMR. J Am Chem Soc 126:6228–6229.
19. Gopalakrishnan K, Bodenhausen G. 2006. Lifetimes of the singlet-states under coherent off-resonance irradiation in NMR spectroscopy. J Magn Reson 182: 254–259.
20. Sarkar R, Vasos PR, Bodenhausen G. 2007. Singlet-state exchange NMR spectroscopy for the study of very slow dynamic processes. J Am Chem Soc 129: 328–334.
21. Sarkar R, Ahuja P, Moskau D, Vasos PR, Bodenhausen G. 2007. Decoupling methods for extending the scope of singlet-state spectroscopy. Chem Phys Chem; in press.
22. Carravetta M, Levitt MH. 2005. Theory of long-lived nuclear spin states in solution nuclear magnetic resonance. I. Singlet states in low magnetic field. J Chem Phys 122:214505–214506.
23. Sorensen OW, Eich GW, Levitt MH, Bodenhausen G, Ernst RR. 1983. Product operator formalism for the description of NMR pulse experiments. Progr Nucl Magn Reson Spectros 16:163–192.
24. Thrippleton MJ, Keeler J. 2003. Elimination of zero-quantum interference in two-dimensional NMR spectra. Angew Chem Int Ed 42:3938–3941.
25. Ahuja P, Sarkar R, Vasos P, Bodenhausen G. 2007. Molecular properties determined from the relaxation of long-lived spin states. J Chem Phys; in press.
26. Cavadini S, Dittmer J, Antonijevic S, Bodenhausen G. 2005. Slow diffusion by singlet state NMR spectroscopy. J Am Chem Soc 127:15744–15748.
27. Balbach J. 2000. Compaction during protein folding studied by real-time NMR diffusion experiments. J Am Chem Soc 122:5887–5888.
28. Reckel S, Lohr F, Dotsch V. 2005. In-cell NMR spectroscopy. ChemBioChem 6:1601–1607.
29. Cohen Y, Avram L, Frish L. 2005. Diffusion NMR spectroscopy in supramolecular and combinatorial chemistry: an old parameter—new insights. Angew Chem Int Ed 44:520–554.

BIOGRAPHIES

Simone Cavadini is a Ph.D. student in the group of Professor Geoffrey Bodenhausen in the Laboratory of Biomolecular Magnetic Resonance in the Chemistry Department at the Swiss Federal Institute of Technology in Lausanne, where in 2005 he received his Master of Science in molecular and biological chemistry. During his Masters project, he explored the application of long-lived states to the study of slow diffusion by NMR. Currently, he is working in the area of solid-state NMR and his research focuses in the development of new methods combining MAS with the indirect detection of ^{14}N via "spy" nuclei with spin $\frac{1}{2}$ such as ^{13}C or ^{1}H.

Paul R. Vasos is a graduate of the University of Bucharest, where he received his degree in Physics. He earned his doctorate in 2004, acquiring the NMR gene from CERM—the Magnetic Resonance Centre at the University of Florence. Subsequently, he has held a postdoctoral position at the University of Maryland. He made the transition back to Europe to join Geoffrey Bodenhausen's team at the Ecole Polytechnique in Lausanne (EPFL), where he is a research assistant. The focus of his research is developing applications to study the dynamics of biological macromolecules, slow conformational exchange and biomolecular folding. Recent research themes include extending the lifetime of the encoded information (spin order) in NMR, using direct detection of low-gamma nuclei (in Florence) and singlet-states (in Lausanne).